FEDSM99-7108

AN EMBEDDED BOUNDARY / VOLUME OF FLUID METHOD FOR FREE SURFACE FLOWS IN IRREGULAR GEOMETRIES

P. Colella, D. T. Graves D. Modiano
Applied Numerical Algorithms Group
Lawrence Berkeley National Laboratory
Berkeley, CA 94720
Email: PColella@lbl.gov, DTGraves@lbl.gov, DLModiano@lbl.gov

Elbridge Gerry Puckett, Mark Sussman
Mathematics Department
University of California, Davis 95616
Email: egp@math.ucdavis.edu, sussman@math.ucdavis.edu

1 ABSTRACT

In this paper, we will present a numerical method for computing incompressible free-surface flows in irregular geometries in three dimensions. The approach we are taking is based on three ideas. The first is the second-order accurate projection method of Bell, Colella, and Glaz (Bell et al., 1989) for computing finite difference approximations to the incompressible flow equations on rectangular grids. The second is the Cartesian grid embedded boundary algorithms of Johansen and Colella (Johansen and Colella, 1998) for computing consistent discretizations of conservation laws in irregular geometries. The third is the use of a second-order accurate volume-of-fluid method for representing the free surface, including the use of a level-set method for computing normals and surface tension.

2 GOVERNING EQUATIONS

We are solving the incompressible Navier-Stokes equations with a given stress tensor (τ). Setting density to unity, the momentum equation becomes

$$\frac{\partial \vec{u}}{\partial t} + (\vec{u} \cdot \nabla)\vec{u} = -\nabla p + \nabla \cdot \tau, \qquad (1)$$

where $\vec{u}$ is the velocity and p is the pressure. We are given an initial condition of the form $\vec{u}(\vec{x}, t = 0)$. Because the density is constant, conservation of mass reduces to constraint upon the velocity field

$$\nabla \cdot \vec{u} = 0. \qquad (2)$$

We are interested in the projection formulation of the equations in which the Hodge decomposition is used to change the problem from a constrained time-dependent system of equations to a pure time-dependent system. The Hodge decomposition states that the any vector field $\vec{W}$ on a bounded domain Ω which satisfies

$$\int_{\partial \Omega} \vec{W} \cdot \hat{n} dA = 0 \qquad (3)$$

can be described as the sum of a divergence free component field ($\vec{W}_d$) and a pure gradient field $\nabla \phi$ (Chorin, 1969).

$$\begin{aligned} \vec{W} &= \vec{W}_d + \nabla \phi \\ \nabla \cdot W_d &= 0 \quad \text{on} \quad \Omega \end{aligned} \qquad (4)$$

where

$$\begin{aligned} W_d \cdot \hat{n} &= 0 \quad \text{on} \quad \partial \Omega \\ \nabla \phi \cdot \hat{n} &= \vec{W} \cdot \hat{n} \quad \text{on} \quad \partial \Omega \end{aligned} \qquad (5)$$

Suppose we have a vector field $\vec{W}$ on a domain Ω and we want to solve for the divergence free component $\vec{W}_d$. If we take the divergence of the equation 4, we can solve

$$\begin{aligned} \nabla^2 \phi &= \nabla \cdot \vec{W} \\ \frac{\partial \phi}{\partial n} &= \vec{W} \cdot \hat{n} \quad on \quad \partial \Omega \end{aligned} \qquad (6)$$

and subtract the pure gradient component

$$\vec{W}_d = \vec{W} - \nabla\phi \qquad (7)$$

to obtain the divergence-free component.

It is convenient to express this process in operator form. We define the projection operator $\mathcal{P}$ to be that operator which extracts the divergence-free component $\vec{W}_d$ of any vector field W.

$$\mathcal{P}\vec{W} = \vec{W}_d \qquad (8)$$

Using $\mathcal{G}$ to be the analytical gradient operator, $\mathcal{I}$ to be the identity operator, and $\mathcal{D}$ to be the divergence operator, the projection operator $\mathcal{P}$ is of the form:

$$\mathcal{P} \equiv (\mathcal{I} - \mathcal{G}(\mathcal{D}\mathcal{G})^{-1}\mathcal{D}). \qquad (9)$$

The projection $\mathcal{P}$ of any pure gradient field therefore vanishes. We can also define the projection operator $\mathcal{Q}$ to be the projection which extracts the pure gradient component field $\nabla\phi$ of any vector field W.

$$\begin{aligned} \mathcal{Q}\vec{W} &= \nabla\phi \\ \mathcal{Q} &\equiv \mathcal{I} - \mathcal{P} \end{aligned} \qquad (10)$$

Partial differential equations whose solutions are constrained by a divergence-free condition can be reformulated with a projection operator to eliminate the constraint. For example, the Navier-Stokes equations (shown in equations 1 and 2) are equivalent to

$$\frac{\partial \vec{u}}{\partial t} = \mathcal{P}(-(\vec{u}\cdot\nabla)\vec{u} + \nabla\cdot\tau) \qquad (11)$$

with a divergence-free initial condition (i.e. $\mathcal{P}(\vec{u}(\cdot, t = 0)) = \vec{u}(\cdot, t = 0)$). Because it is a purely spacial operator, the projection operator $\mathcal{P}$ commutes with the time derivative. The pressure gradient is no longer necessary as the projection of any pure gradient vanishes. We shall refer to equation 11 as the "projection formulation" of the Navier-Stokes equations.

3 DISCRETIZATION

The problem domain is discretized as a uniform Cartesian grid with unit aspect ratio, with an irregular domain boundary embedded in the grid. The grid cells and faces that the boundary intersects are represented with irregular geometry data. The cells and faces that do not intersect the boundary have uniform geometric properties. For clarity of exposition, this paper is written as if each grid cell or face contains no more than one irregular cell or face, so that the familiar ijk index notation is used throughout the grid. Cells have integer indices and faces have one half-integer index.

For this algorithm, the segment of the boundary internal to an irregular cell is modeled as a planar surface. As shown in figure 1, the geometry of an irregular cell is completely defined by Λ, the fraction of its volume that is inside the problem domain, and by $\vec{n}_b$, the vector normal to the boundary segment. The geometry of an irregular face is defined by ℓ, the fraction of its area that is inside the problem domain. From these data, other geometric properties can be constructed, such as the centroid locations of irregular cells or edges.

The solution is represented as a set of average values within each cell. Geometrically, we consider the average to be located at the center of the regular grid cell, even in irregular cells where it might seem more natural for the solution to be located at the centroid. Note that in cells with volume fraction less than one-half, this results in the data being located outside the problem domain.

This method requires the solution of several Poisson-like problems. The discrete Laplacian operator is a composition of discrete gradient and divergence operators. The gradient operator acts on cell-centered data and approximates the gradient at the centers of the regular grid faces. There is no influence of the geometry. The divergence operator acts on face-centered data and approximates the divergence at the centroid of a cell. The divergence operator includes a transformation of data at the centers of regular grid faces into data at the centroids of irregular faces. This is explained in detail in section 3.1.2.

3.1   Discrete Laplacian operator

The discrete Laplacian operator $\mathbf{L}$ is the composition of discrete gradient and divergence operators. In the irregular cells, it is evaluated using a finite volume discretization of the divergence of an edge-centered flux term that in this case is equal to the gradient times the face area. On the regular grid, the Laplacian reduces to the usual five- (or seven-) point cross-shaped stencil, and is evaluated directly.

3.1.1   Discrete gradient operator. The gradient operator $\overline{\mathbf{G}}$ takes cell-centered data and produces edge-centered gradients. There is no influence of geometry, so the same formula is used for every face that intersects the problem

2   Copyright © 1999 by ASME

domain. The gradient normal to the face $(i + 1/2, j, k)$ is

$$g^x_{i+1/2,j,k} = \mathbf{G}^x(\phi)|_{i+1/2,j,k}$$
$$= \frac{\phi_{i+1,j,k} - \phi_{ijk}}{h}$$

and the gradient tangential to the face is formed from an average of the other set of normal gradients:

$$g^y_{i+1/2,j,k} = \mathbf{G}^y(\phi)|_{i+1/2,j,k}$$
$$= \frac{g^y_{i,j+1/2,k} + g^y_{i+1,j+1/2,k} + g^y_{i,j-1/2,k} + g^y_{i+1,j-1/2,k}}{4}$$
$$= \frac{\phi_{i,j+1,k} - \phi_{i,j-1,k} + \phi_{i+1,j+1,k} - \phi_{i+1,j-1,k}}{4h}$$

and similarly for the other combinations of gradient direction and face direction.

The gradient at faces outside the problem domain are formed by extrapolation. For example,

$$g^x_{i+1/2,j,k} = 2\, g^x_{i-1/2,j,k} - g^x_{i-3/2,j,k}.$$

3.1.2 Discrete divergence operator.
The finite-volume form of the divergence operator $\mathbf{D}$ is

$$\mathbf{D}_{ijk} = \frac{1}{\Lambda_{ijk} h} \left\{ \ell^b_{ijk} F^b_{ijk} \right.$$
$$- \left(\ell_{i+1/2,j,k} F^x_{i+1/2,j,k} - \ell_{i-1/2,j,k} F^x_{i-1/2,j,k} \right)$$
$$- \left(\ell_{i,j+1/2,k} F^y_{i,j+1/2,k} - \ell_{i,j-1/2,k} F^y_{i,j-1/2,k} \right)$$
$$\left. - \left(\ell_{i,j,k+1/2} F^z_{i,j,k+1/2} - \ell_{i,j,k-1/2} F^z_{i,j,k-1/2} \right) \right\} \quad (12)$$

where $F_{(x,y,z)} = \ell g^{(x,y,z)}$ are fluxes at the faces of the cell, F^b is the flux normal to the irregular segment of the boundary, Λ_{ijk} is the fraction of the volume of the regular cell taken up by the irregular cell, $\ell_{i+1/2,j,k}$ *etc.* are the area fractions of the irregular faces of the cell, and ℓ^b is the length of the irregular segment of the boundary.

We define the solution data in an irregular cell to be located at the center of the appropriate regular grid grid cell, not at the centroid of the irregular volume. Thus, the fluxes computed at the centers of the grid faces are second order. However, to compute a second order flux divergence in the irregular cells, the fluxes in equation 12 must be centered at the geometric centroids of the faces. We therefore adopt the idea introduced by Johansen and Colella (Johansen and Colella, 1998), to linearly interpolate the second order fluxes to the centroids of the faces. In figure 2, the regular grid spacing is h, and the centroids of the faces are offset from the centers of the grid faces by $(\xi^c h, \eta^c h, \zeta^c h)$. If $\widetilde{F}$ are the second order fluxes at the centers of the grid faces and F are the fluxes at the centroids of the irregular faces, then

$$F_{i+1/2,j} = \left(1 - \eta^c_{i+1/2,j} \right) \widetilde{F}_{i+1/2,j} + \eta^c_{i+1/2,j} \widetilde{F}_{i+1/2,j+1}$$

in two dimensions and

$$F_{i+1/2,j,k} = \left(1 - \eta^c_{i+1/2,j,k} - \zeta^c_{i+1/2,j,k} \right) \widetilde{F}_{i+1/2,j,k}$$
$$+ \eta^c_{i+1/2,j,k} \widetilde{F}_{i+1/2,j+1,k} + \zeta^c_{i+1/2,j,k} \widetilde{F}_{i+1/2,j,k+1}$$

in three dimensions.

3.2 Time Discretization
To advance the solution in time, we employ a variation of the time discretization used by Bell, Colella, and Glaz (Bell et al., 1989). It is a two-step algorithm. First we create a temporary velocity $\vec{u}^*$ by advancing the solution using the governing equations but ignoring the divergence constraint.

$$\vec{u}^* = \vec{u}^n + \Delta t \left(-\vec{u} \cdot \nabla \vec{u}^{n+\frac{1}{2}} - \nabla p^{n-\frac{1}{2}} - \frac{1}{2} \mathbf{D}(\tau^n + \tau^*) \right) \quad (13)$$

where τ^n is the stress tensor evaluated using velocity $\vec{u}^n$ and τ^* is the stress tensor evaluated using velocity $\vec{u}^*$. Equation 13 therefore requires the solution of a linear system whose form depends on the form of the stress tensor. We then enforce the incompressibility constraint and update the pressure gradient by using the discrete projection operators P and Q.

$$\frac{\vec{u}^{n+1} - \vec{u}^n}{\Delta t} = \mathbf{P} \left(-\vec{u} \cdot \nabla \vec{u}^{n+\frac{1}{2}} - \frac{1}{2} \mathbf{D}(\tau^n + \tau^*) \right)$$

$$\nabla p^{n+\frac{1}{2}} = \mathbf{Q} \left(-\vec{u} \cdot \nabla \vec{u}^{n+\frac{1}{2}} - \frac{1}{2} \mathbf{D}(\tau^n + \tau^*) \right)$$

3.3 Predictor
We compute the advective term $(\vec{u} \cdot \nabla \vec{u})^{n+1/2}$ following Almgren, Bell, Colella and Marthaler (Almgren et al.,

1997). We linearize the advective portion of the flow equations, construct van Leer-limited slopes at the cells, and extrapolate by a half time step and a half the grid spacing to form values at the faces. We then perform an exact discrete projection

$$\mathbf{P} = \mathbf{I} \ - \ \mathbf{G}\mathbf{L}^{-1}\mathbf{D}$$

using $\mathbf{G}$ and $\mathbf{D}$ as described in section 3.1.1 and 3.1.2. The Poisson problem has von Neumann boundary conditions, which is implemented by setting the flux F_b normal to the embedded boundary segment in eqn. 12 to zero. It is solved using multigrid iteration. We construct the advective term directly, not in conservative form.

3.4 Diffusion operator

In the case where $\tau = \nu \nabla u$, equation 13 can be rearranged to form

$$\left(\mathbf{I} - \tfrac{1}{2}\nu\,\Delta t\nabla^2\right)\vec{u}^{\star} =$$
$$\vec{u}^n - \Delta t \left[(\vec{u}{\cdot}\nabla\vec{u})^{n+1/2} - \tfrac{1}{2}\nabla^2\vec{u}^n + \nabla p^{n-1/2}\right]$$

where the face-centered advection term $(\vec{u}\nabla\vec{u})^{n+1/2}$ is computed as described in section 3.3. As with Poisson's equation, we solve the diffusion equation using multigrid iteration. The major complication is the no-slip boundary, which introduces a Dirichlet boundary condition and a non-zero flux at the embedded boundary. We adopt the method of Johansen and Colella (Johansen and Colella, 1998), to quadratically reconstruct the solution along a ray normal to the boundary segment to find the normal gradient at the boundary.

3.5 Cell-centered projection

The solution at the new time level is given by the projection

$$\vec{u}^{n+1} = \mathbf{P}\left(\vec{u}^{\star} + \Delta t\,\nabla p^{n-1/2}\right).$$

Both the argument and the result of the projection are cell-centered. In order to construct the right hand side of Poisson's equation, and the correction to the velocity, we define the cell-centered gradient and divergence operators $\mathbf{G}^{CC}$ and $\mathbf{D}^{CC}$ as the composition of the face-centered operators $\mathbf{D}$ and $\mathbf{G}$ with the averaging operators $\mathbf{A}^{F\to C}$ and $\mathbf{A}^{C\to F}$, which, respectively, average face-centered data to cells, and

cell-centered data to edges.

$$\mathbf{G}^{CC}(\phi) = \mathbf{A}^{F\to C}(\mathbf{G}(\phi))$$
$$\mathbf{D}^{CC}(\vec{u}) = \mathbf{D}(\mathbf{A}^{C\to F}(\vec{u}))$$

If we construct a Laplacian $\mathbf{L}^{CC} = \mathbf{D}^{CC}\mathbf{G}^{CC}$, we obtain a decoupled stencil. Therefore, we perform an approximate cell-centered projection using the Laplacian operator constructed from the edge-centered gradient and divergence operators,

$$\mathbf{P}^{CC} = \mathbf{I} \ - \ \mathbf{G}^{CC}\mathbf{L}^{-1}\mathbf{D}^{CC}.$$

Because $\mathbf{L} \neq \mathbf{D}^{CC}\mathbf{G}^{CC}$, this projection is approximate.

4 MODIFICATION OF CONSTANT DENSITY ALGORITHM FOR MULTI-FLUID FLOW

We modify the equations for constant density flow (1) as follows:

$$\frac{\partial \vec{u}}{\partial t} + (\vec{u} \cdot \nabla)\vec{u} = -\frac{\nabla p}{\rho} + \frac{\nabla \cdot 2\mu\tau}{\rho} - \frac{\gamma\kappa\nabla H}{\rho} \qquad (14)$$

$$\frac{\partial \phi}{\partial t} + (\vec{u} \cdot \nabla)\phi = 0 \qquad (15)$$

$$\frac{\partial F}{\partial t} + (\vec{u} \cdot \nabla)F = 0. \qquad (16)$$

The above formulation is the level set formulation for multi-fluid flow (Sussman et al., 1994; Chang et al., 1996). The provisional variable ϕ represents the signed distance to the free surface. The variable F represents the volume fraction of liquid contained in any one computational cell. The density $\rho(\phi)$, viscosity $\mu(\phi)$, and Heaviside function $H(\phi)$ jump across the free surface (where ϕ changes sign). γ is the surface tension coefficient. Since the density ρ is non-constant, we implement a variable density projection method (Bell and Marcus, 1992) which is a generalization of 4. Given a vector field $\vec{W}$, we decompose it into a divergence free part $\vec{W}_d$ and the gradient of a scalar divided by density $\nabla p/\rho$.

The location of the fluid interface is advanced in time using a coupled volume-of-fluid / level set algorithm (Sussman and Puckett, 1998). In this algorithm the flux of each fluid across cell edges during a time step is computed from a second-order accurate, piecewise linear approximation to the interface. This representation of the interface is constructed from the volume fraction of each fluid in each cell at the current time step and the unit normal to the interface obtained from the level set function at that time step. The

volume fractions in each cell at the new time step are computed using a conservative finite difference update, while a provisional level set function at the new time step is obtained by solving an advection equation for the level set function. This information at the new time step is used to obtain a piecewise linear approximation to the interface at the new time, which in turn is used to construct a distance function (i.e., the level set function) at the new time. This distance function is then used to compute the unit normal and curvature of the interface. This information is used to compute the surface tension forces and the volume fluxes at the next time step.

5 EXAMPLES

We present two examples. The first, is a constant density flow past a half-cylinder. The second, is a free surface flow through a nozzle.

The flow past a half cylinder has been computed in the work of (Almgren et al., 1997) using a "nodal" projection formulation and also by (Almgren et al., 1995) using a "cell centered" projection formulation. As described above, our numerical method is based on a "cell centered" projection. One difference between this work and previous work by (Almgren et al., 1995) is the incorporation of a second order algorithm for computing the divergence of an edge based velocity field at the embedded boundary. The resolution of our calculation is 256×64, the domain is 4×1, and the diameter of the half cylinder is 0.25. At inflow, we enforce $U = 1$ and we have outflow boundary conditions imposed on the right edge of the domain. The initial conditions are defined by the projection of a uniform inlet velocity and quiescent fluid with a slight asymmetric perturbation upstream of the obstruction. In figure 3 we display a snapshot of vorticity being shed from the half cylinder.

For our second example, we compute the three dimensional flow of water jetting into air. The motion of the free-surface separating the liquid from the gas is modeled using the "coupled levelset and volume of fluid" algorithm described in (Sussman and Puckett, 1998). In Figure 4 we display preliminary results of liquid being ejected from a nozzle. The liquid is accelerated out of the nozzle by applying a pressure boundary condition at the base of the nozzle which mimics the effects of a thermal ink-jet device. The diameter of the nozzle is 12 microns and the length of the nozzle is 36 microns. The surface tension coefficient is $37 dynes/cm$ and the density ratio is $100 : 1$.

REFERENCES

Almgren, A. S., Bell, J. B., Colella, P., and Marthaler, T. (1995). A cell-centered cartesian grid projection method
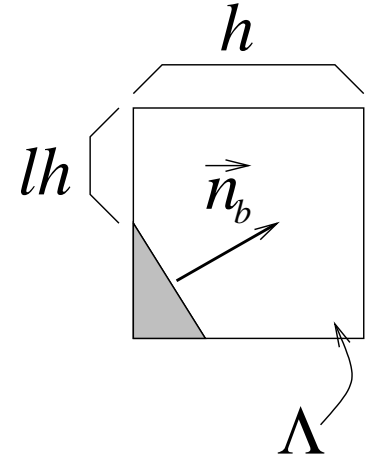
Figure 1.   Geometry parameters. Shaded areas are solid. Λ = volume fraction, ℓ = face area fractions, $\hat{n}$ = boundary segment unit normal.
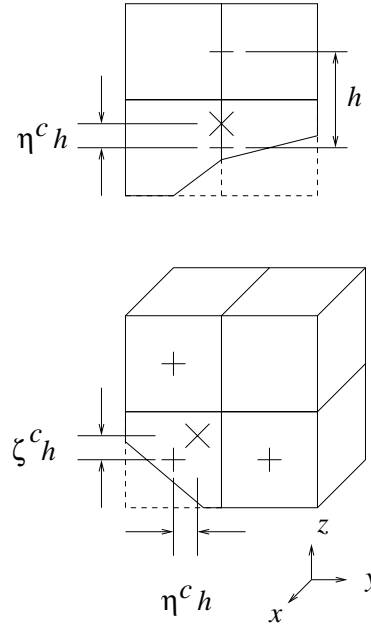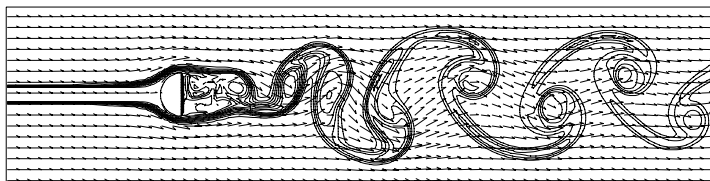

Figure 2.   Flux interpolation. Given fluxes at grid face centers (+), linearly interpolate to face centroid ($\times$).

1500 steps

Figure 3. Vortex shedding past a half-cylinder in a channel; contours of a passive scalar are displayed.

for the incompressible euler equations in complex geometries. AIAA Paper 95-1743-CP, in *Proceedings of the AIAA 12th Computational Fluid Dynamics Conference.*

Almgren, A. S., Bell, J. B., Colella, P., and Marthaler, T. (1997). A cartesian grid projection method for the incompressible euler equations in complex geometries. *SIAM J. Sci. Comp.*, 18(5).

Bell, J. B., Colella, P., and Glaz, H. M. (1989). A second-order projection method for the incompressible Navier-Stokes equations. *J. Comput. Phys.*, 85:257–283.

Bell, J. B. and Marcus, D. L. (1992). A second-order projection method for variable-density flows. *J. Comp. Phys.*, 101:334–348.

Chang, Y., Hou, T., Merriman, B., and Osher, S. (1996). Eulerian capturing methods based on a level set formulation for incompressible fluid interfaces. *J. Comp. Phys.*, 124:449–464.

Chorin, A. J. (1969). On the convergence of discrete approximations to the Navier-Stokes equations. *Math. Comp.*, 23:341–353.

Johansen, H. and Colella, P. (1998). A cartesian grid embedded boundary method for poisson's equation on irregular domains. *J. Comput. Phys.*, 147(1):60–85.

Sussman, M. and Puckett, E. (1998). A coupled level set and volume of fluid method for computing 3d and and axisymmetric incompressible two-phase flows. *J. Comp. Phys.* submitted.
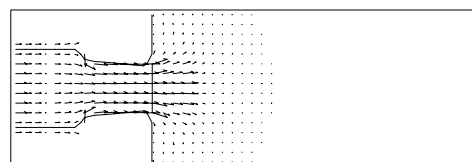
Sussman, M., Smereka, P., and Osher, S. (1994). A level set approach for computing solutions to incompressible two-phase flow. *J. Comp. Phys.*, 114:146–159.
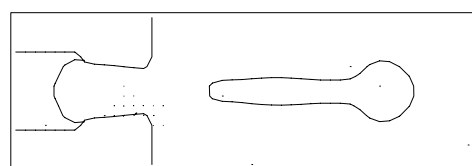
t=9 microseconds
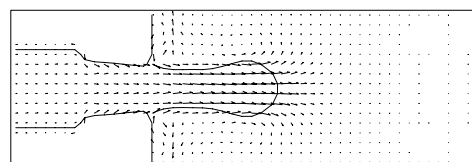
t=4 microseconds

t=0

Figure 4. 2-d slice in y-z plane of a 3d jetting computation. The density ratio at the free surface is 100:1 and the surface tension coefficient is 37 dynes/cm. Viscous effects are ignored in this computation.